



1,3-Dialkyl-8-N-substituted benzyloxycarbonylamino-9-deazaxanthines as potent adenosine receptor ligands: Design, synthesis, structure–affinity and structure–selectivity relationships

Franco Fernández^a, Olga Caamaño^a, M. Isabel Nieto^a, Carmen López^a, Xerardo García-Mera^a, Angela Stefanachi^c, Orazio Nicolotti^c, M. Isabel Loza^b, Jose Brea^b, Cristina Esteve^d, Victor Segarra^d, Bernat Vidal^d, Angelo Carotti^{c,*}

^a Departamento de Química Orgánica, Facultad de Farmacia, Universidade de Santiago de Compostela, 15782 Santiago de Compostela, Spain

^b Departamento de Farmacología, Instituto de Farmacia Industrial, Universidade de Santiago de Compostela, 15782 Santiago de Compostela, Spain

^c Dipartimento Farmaco-chimico, Università degli Studi di Bari, via Orabona 4, I-70125 Bari, Italy

^d Medicinal Chemistry Department, Laboratorios Almirall, S.A., E-08960 St. Just Desvern, Barcelona, Spain

ARTICLE INFO

Article history:

Received 9 February 2009

Revised 30 March 2009

Accepted 31 March 2009

Available online 5 April 2009

Keywords:

9-Deazaxanthines

Carbamates

Adenosine receptors (ARs)

Adenosine receptor antagonists

ABSTRACT

A number of 1,3-dialkyl-9-deazaxanthines (9-dAXs), bearing a variety of N-substituted benzyloxycarbonylamino substituents at position 8, were prepared and evaluated for their binding affinity to the recombinant human adenosine receptors (hARs), chiefly to the hA_{2B} and hA_{2A} AR subtypes. Several ligands endowed with excellent binding affinity to the hA_{2B} receptors, but low selectivity versus hA_{2A} and hA_1 were identified. Among these, 1,3-dimethyl-N-3'-thienyl carbamate **15** resulted as the most potent ligand at hA_{2B} ($K_i = 0.8$ nM), with a low selectivity versus hA_{2A} ($hA_{2A}/hA_{2B} = 12.6$) and hA_1 ($hA_1/hA_{2B} = 12.5$) and a higher selectivity versus hA_3 ($hA_3/hA_{2B} = 454$). When tested in functional assays in vitro, compound **15** exhibited high antagonist activities and efficacies versus both the A_{2A} and A_{2B} receptor subtypes, with pA_2 values close to the corresponding pK_i s. A comparative analysis of structure–affinity and structure–selectivity relationships of the similar analogues 8-N-substituted benzyloxycarbonylamino- and 8-N-substituted phenoxyacetamido-9-dAXs suggested that their binding modes at the hA_{2B} and hA_{2A} ARs may strongly differ. Computational studies help to clarify this striking difference arising from a simple, albeit crucial, structural change, from CH_2OCON to OCH_2CON , in the *para*-position of the 8-phenyl ring. © 2009 Elsevier Ltd. All rights reserved.

1. Introduction

Adenosine is an endogenous purine nucleoside that mediates several important physiological effects by activating four diverse G protein-coupled adenosine receptors (ARs), named A_1 , A_{2A} , A_{2B} and A_3 .¹ The medicinal chemistry, pharmacology and potential therapeutic applications of subtype selective AR ligands have been extensively reviewed.^{2–4}

In the search for new antiasthmatic drugs we have been targeting A_{2B} AR antagonists based on the observation that the bronchodilating activity of two xanthinic drugs, that is, theophylline and enprofylline, might be ascribed to selective, albeit small, antagonism versus the A_{2B} AR subtype.^{5,6} Since activation of A_{2B} ARs stimulates vasodilation, cardiac fibroblast proliferation, hepatic glucose and interleukin-6 biosynthesis and Cl^- secretion in intestinal epithelia, it can be hypothesized that potent and selective A_{2B} AR antagonists might be used in many other pathologies,

for example Alzheimer's disease, cystic fibrosis and type-II diabetes.²

Several groups have designed and tested many xanthine derivatives aiming at the discovery of new, potent and A_{2B} -selective ligands.^{3,4,7–9} Good results have been initially obtained by Jacobson and co-workers who described many xanthine derivatives, such as XAC (**1**)¹⁰ and MRS1754 (**2**)¹¹ (Chart 1) that were endowed with high affinity and selectivity versus the A_{2B} AR. Along this line of research, we recently reported the design, synthesis, structure–activity (SAR) and structure–selectivity (SSR) relationships of a large series of 9-deazaxanthines (9-dAXs) and 9-OH-9-dAXs,^{12–16} two poorly exploited classes of xanthine analogues, bearing the same 8-N-substituted-phenoxyacetamido moiety proposed by Jacobson. In contrast with the biological data reported for 9-dAXs differently substituted at position 8,^{17,18} these compounds showed both higher affinity and selectivity versus the hA_{2B} AR (see compounds **3**,¹⁴ **4**,¹⁴ and **5**¹⁶ in Chart 1).

Similar results were obtained by other groups for differently 8-substituted xanthines (e.g., compound **6**¹⁹) and 9-dAX (e.g., compound **7**²⁰).

* Corresponding author. Tel.: +39 080 5442782; fax: +39 080 5442230.
E-mail address: carotti@farmchim.uniba.it (A. Carotti).

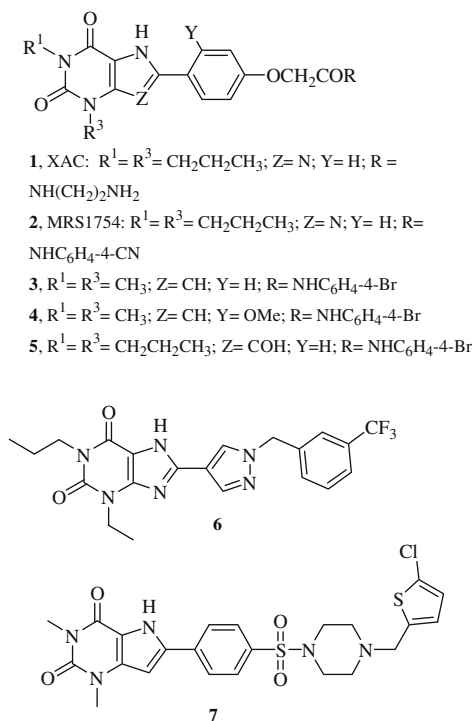


Chart 1. Xanthine and 9-dAX derivatives with potent and selective antagonist activities versus the A_{2B} AR subtype.

To further extend the SAR study of 9-dAXs as AR ligands and identify a new class of selective A_{2B} AR antagonists, we designed a series of 1,3-dialkyl-8-N-substituted benzyloxycarbonylamino-9-dAXs (Chart 2) by replacing the phenoxyacetamido group at position 8 in compounds **3** and **4** with a benzyloxycarbonylamino group. Synthesis, biological evaluation, and SAR and SSR studies of this new class of AR ligands were the objectives of the present study.

2. Chemistry

Synthesis of the target compounds 1,3-dialkyl-8-substituted-9-dAX carbamates, (1,3-dialkyl-2,4-dioxo-1*H*-pyrrolo[3,2-*d*]pyrimidin-6-yl)phenyl)methylcarbamates), **13–32**, performed according to published procedures,^{14,21–23} is outlined in Scheme 1. First, the condensation of uracil derivatives **8** with *para*-substituted benzaldehydes **9** afforded the appropriate 6-styryluracils **10**, which were treated with sodium dithionite in formic acid under reflux to undergo a reductive cyclization to the corresponding 9-dAX derivatives **11**.

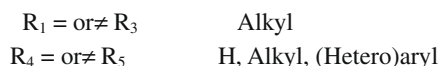
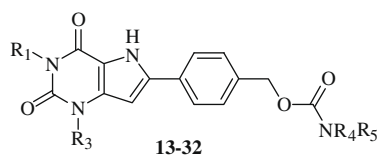


Chart 2. General structure and main structural variations of 1,3-dialkyl-8-N-substituted benzyloxycarbonylamino-9-dAX AR ligands **13–32**.

Yields in the cyclization products varied considerably depending on the starting 6-styryluracil, that is, high for the carboxyphenyl derivatives **11a** (80%) and **11b** (90%) and dramatically reduced for **11d** (18%) and the (hydroxymethyl)phenyl derivative **11c** (17%), which was obtained as formate. Reduction of the carboxylic group of **11a, b, d** with $\text{BH}_3 \cdot \text{THF}$ afforded the corresponding 9-dAX alcohols **12**. Conversion of intermediates **12** to the target compounds **13–32** was achieved by employing different methods (Scheme 1). The first carbamate formation procedure (method A) involved the reaction of the corresponding 9-dAX alcohol **12** with an excess of the appropriate isocyanate in DMF at 115 °C. In the second procedure (method B), the 9-dAX alcohol was treated with the appropriate isocyanate in dioxane at reflux. The third procedure (method C) involved the formation of an intermediate imidazolidine, by reaction of the alcohols **12** with *N,N'*-carbonyldiimidazole (CDI) in pyridine,²⁴ followed by a reaction with the adequate amine.²⁵

3. Biochemical and pharmacological assays

Affinity of compounds **13–32** to human A_1 , A_{2A} , A_{2B} and A_3 ARs was evaluated as described in our previous investigations.^{13–16} All active compounds fully displaced the specific binding of radioligands to receptors in a concentration-dependent manner; slopes were not significantly different from unity at the 5% level of statistical significance (Fig. 1). High antagonist activity of ligand **15** was measured by means of isolated organ assays at rat colon A_{2B} (Fig. 2) and rat aorta A_{2A} AR subtypes. The compound concentration-dependently displaced the curves of the AR agonist NECA to the right in a parallel way without lowering their maximum, in good agreement with a competitive antagonism.

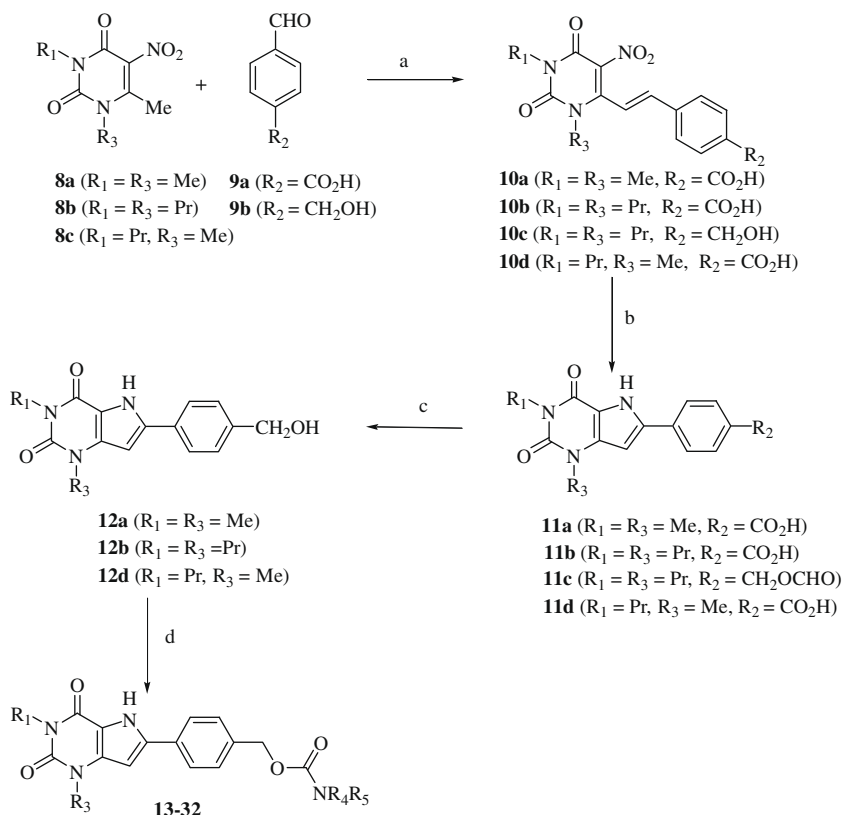
4. Results and discussion

4.1. SAR and SSR studies

Chemical structures and human AR binding affinities of the examined ligands are reported in Table 1. Binding affinity values are the means of two independent experiments performed with duplicate points. SEM values were always lower than 10%. It must be kept in mind that the main goal of our investigation was to discover new and highly potent hA_{2B} antagonists^{13–16} endowed with good selectivity versus hA_{2A} , as measured by the selectivity index (SI) which is the ratio $K_i hA_{2A}/K_i hA_{2B}$. Since most of the ligand binding affinities to both the hA_{2B} and hA_{2A} ARs turned to be good and rather close, resulting in very low SIs (see Table 1), the affinities to hA_1 and hA_3 ARs were determined only for parent compounds and for ligands with high hA_{2B} affinity or relatively high SI. In Table 1, only the percentage of radioligand displacement at 1 μM was reported for low active compounds or for compounds whose low solubility prevented the determination of their K_i .

For a more immediate and efficient analysis of the SAR and SSR, binding data were presented graphically as a plot of $\text{p}K_i hA_{2A}$ (*Y*-axis) versus $\text{p}K_i hA_{2B}$ (*X*-axis) using the same scale and range for both axes (square plot in Fig. 3); note that for the affinity of ligand **29** at hA_{2B} an estimated $\text{p}K_i = 6.05$ was used. On the bisector of the plot ($Y = X$) compounds with equal affinities at both ARs are located, whereas highly hA_{2B} -selective compounds are observed far below the bisector. The distance of their $\text{p}K_i$ values from the bisector line is a direct measure of the degree of selectivity: the greater the distance the higher the SI values in Table 1.

At a glance, binding data in Figure 3 reveal that ligands with good affinities for both the hA_{2B} and hA_{2A} AR subtypes were obtained. Indeed, 14 of 20 newly synthesized compounds, comprised



Scheme 1. Reagents and conditions: (a) piperidine, dioxane, Δ ; (b) HCO_2H , $\text{Na}_2\text{S}_2\text{O}_4$, reflux; (c) $\text{BH}_3\cdot\text{THF}$ 1 M, THF, 0 °C, then rt; (d) Method A: R_4NCO , DMF, 115 °C; Method B: R_4NCO , dioxane, 100 °C; Method C: CDI, $\text{R}_4\text{R}_5\text{NH}$, pyridine, rt.

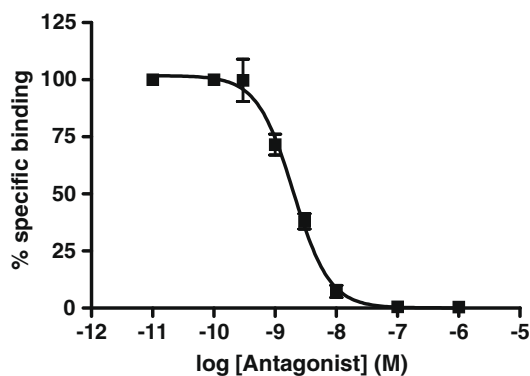


Figure 1. Binding competition experiments at cloned hA_{2B} ARs. Concentration-response curve for compound **15**. Values represent the means \pm SEM (vertical bars) of two independent experiments.

in the cyan-highlighted area of the plot, yielded a $pK_i > 6.85$ ($K_i < 140$ nM).

The 1,3-dimethyl-*N*-3'-thienyl-carbamate **15** resulted as the most potent ligand displaying a sub-nanomolar binding affinity to the hA_{2B} AR ($K_i = 0.8$ nM) whereas its *N*-2'-thienyl isomer **16** exhibited the second highest affinity to the same hA_{2B} AR ($K_i = 1$ nM). Ligands with the highest affinity to the hA_{2A} AR were the 1,3-dimethyl-*N*-3'-thienyl carbamate **15** ($K_i = 10.5$ nM) and the 1,3-dipropyl-*N*-3'-pyrazolyl-carbamate **28** ($K_i = 10$ nM). The lowest affinities to both the hA_{2B} and hA_{2A} ARs were displayed by the 1,3-dipropyl-*N*-thienyl derivatives **24** and **25** ($K_i = 501$ and 602, and 3311 and 2240 nM, to hA_{2B} and hA_{2A} ARs, respectively).

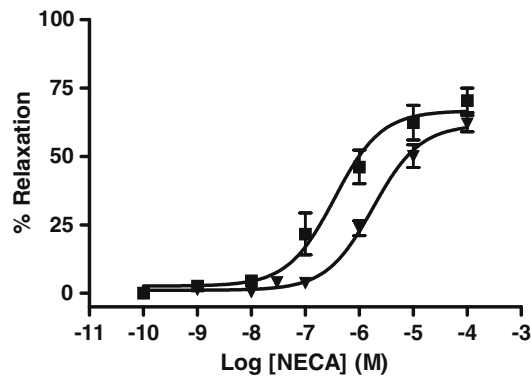


Figure 2. Isolated organ assays for rat A_{2B} receptors. Cumulative concentration-response curves to NECA in the absence (\blacksquare) and in the presence (\blacktriangle) of **15** at 10 nM concentration. Points represent the means \pm SEM (vertical bars) of two independent assays ($n = 2$).

Noticeably, all the ligands tested for the hA_1 AR subtype exhibited a low nanomolar activity, being the 1,3-dipropyl-*N*-*p*-F-phenyl derivative **23** the most potent ligand with a $K_i = 0.4$ nM. Analysis of selectivity data in the plot, that is, the distances of pK_i values from the bisector line, revealed that no ligand exhibited a substantial selectivity versus the hA_{2B} AR. Indeed, the highest SIs were 61.6 and 50.0 for the 1,3-dimethyl-*N*-benzyl derivative **21** and the 1,3-dipropyl-*N*-*p*-F-phenyl derivative **23**, respectively. These discouraging findings prompted us to synthesize and test the 1-propyl-3-methyl-9-dAX carbamate **32** designed on the basis of the increased selectivity versus hA_{2B} observed in 8-*N*-substituted phenoxylacetamido-9-dAXs^{14–16} and -xanthines,^{11,26} bearing larger

Table 1Chemical structures and *h*AR binding affinities^a of 1,3-dialkyl-8- N-substituted benzyloxycarbonylamino-9-dAX derivatives **13–32**

Compound	Structure	<i>K</i> _i <i>hA</i> _{2B}	<i>K</i> _i <i>hA</i> _{2A}	SI ^b	<i>K</i> _i <i>hA</i> ₁ ^c	<i>K</i> _i <i>hA</i> ₃ ^c
13		2.8	34.7	12.6	2.2	275
14		9.5	72.4	7.6	17.8	871
15^d		0.8	10.5	12.6	10.0	363
16		10	15.1	15.1	nd	nd
17		81.3	490	6.0	nd	nd
18		3.2	18.2	5.6	nd	nd
19		11.5	132	11.5	nd	nd
20		2.1	43.7	20.4	nd	nd

(continued on next page)

Table 1 (continued)

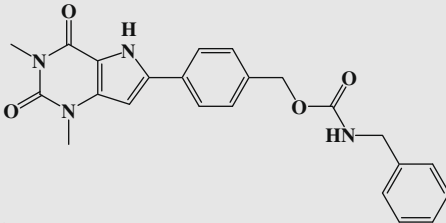
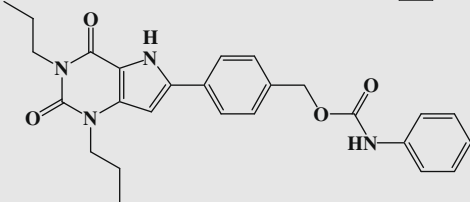
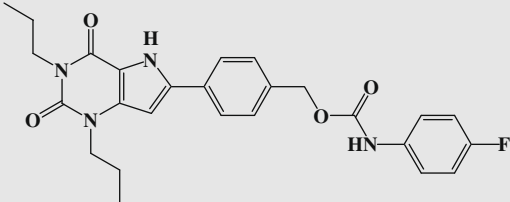
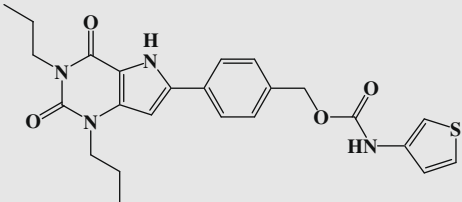
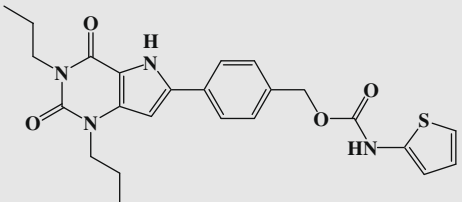
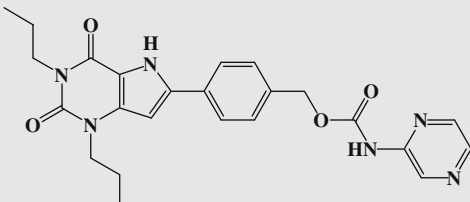
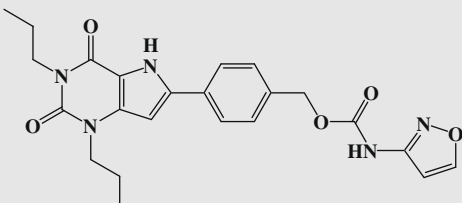
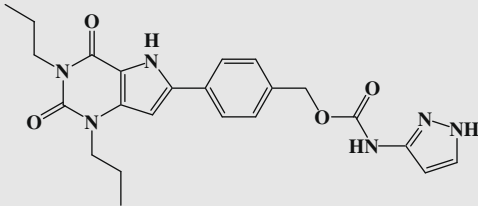
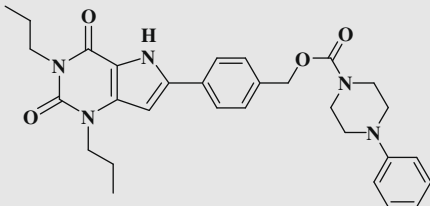
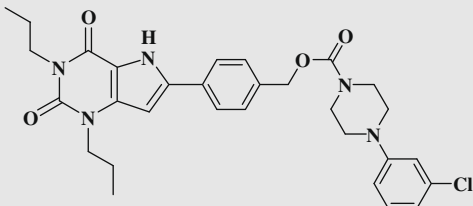
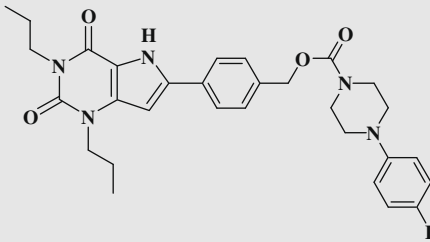
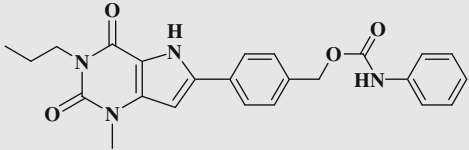
Compound	Structure	K_i hA _{2B}	K_i hA _{2A}	SI ^b	K_i hA ₁ ^c	K_i hA ₃ ^c
21		16.2	1000	61.6	nd	nd
22		7.1	28.8	4.1	20.4	331
23		2.0	118	59	0.4	71
24		501	3311	6.6	nd	nd
25		602	2240	3.7	nd	nd
26		7.8	35.5	4.6	nd	nd
27		1.7	21.9	12.9	nd	nd

Table 1 (continued)

Compound	Structure	K_i hA_{2B}	K_i hA_{2A}	SI ^b	K_i hA_1 ^c	K_i hA_3 ^c
28		5.9	10.0	1.7	nd	nd
29		46% ^e	447	—	nd	nd
30		24.0	28.2	1.2	nd	nd
31		42.7	50.1	1.2	nd	nd
32		13.8	15%	—	nd	nd

^a Affinity values to the indicated human cloned ARs are expressed as K_i (nM) or as % of inhibition at a 1 μ mol concentration. SEMs from two independent experiments were always lower than 10%.

^b SI is the selectivity index defined as the ratio K_i hA_{2A}/K_i hA_{2B} .

^c nd stands for not determined.

^d In functional assays, compound **15** exhibited the following antagonist potency: pA_2 A_{2B} (rat) = 8.66 ± 0.30 , pA_2 A_{2A} (rat) = 7.55 ± 0.19 .

^e An estimated K_i equal to 900 nM was used in the plot of Figure 3.

alkyl substituents at position 1 than at position 3. Ligand **32** maintained a good affinity to the hA_{2B} AR (K_i = 13.8 nM) close to that exhibited by the two corresponding symmetrically substituted parent compounds **13** and **22** (K_i = 2.8 and 7.1 nM, respectively) but, unfortunately, its low solubility allowed only the determination of the % of radioligand displacement at the hA_{2A} AR at 1 μ M concentration. Eventhough the low percentage of inhibition (15%) might be indicative of a K_i » 1000 nM, a secure assessment of the hA_{2B} selectivity was not possible.

A comparative analysis of affinity and selectivity data of 1,3-dimethyl- and 1,3-dipropyl-9-dAXs pointed out some interesting trend. With few exceptions, 1,3-dimethyl-9-dAX carbamates exhibited higher hA_{2B} affinities than the corresponding 1,3-dipropyl analogues (see plot in Fig. 4). The most striking, and unexpected-

edly high, increase of K_i was observed for the *N*-3'-thienyl (compare **15** with **24**) and the *N*-2'-thienyl (compare **16** with **25**) carbamates from 0.8 to 501 and from 1 to 602 nM, respectively. These data differ considerably from those obtained for the 8-*N*-substituted phenoxyacetamido-9-dAX analogues^{14,15} and might suggest a significantly diverse binding mode of the 1,3-dialkyl substituents in the two diverse classes of 8-*p*-substituted phenyl-9-dAXs. The observation that 9-dAX carbamates yielded very low SI values, arising from an unexpectedly high affinity to the hA_{2A} AR subtype, sharply contrasts with the high K_i hA_{2A}/K_i hA_{2B} SI elicited by the 8-*N*-substituted phenoxyacetamido-9-dAX analogues.^{14,15} Furthermore, it lends additional support to the hypothesis of a different binding mode for the hA_{2B} and more so for the hA_{2A} AR subtypes.

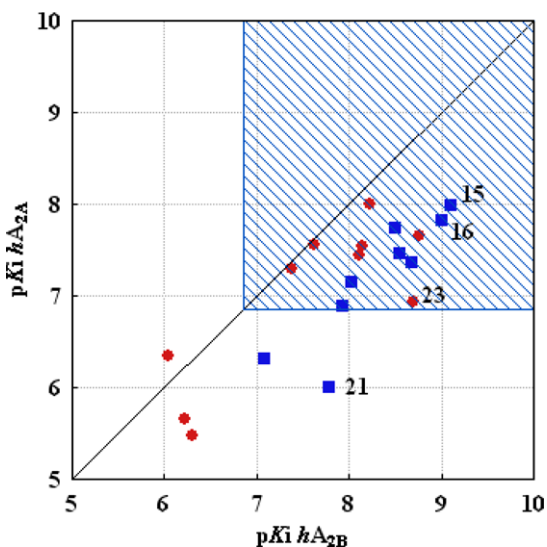


Figure 3. Affinity-selectivity plot of 9-dAX AR ligands **13–32**. Blue squares and red circles indicate 1,3-dimethyl- and 1,3-dipropyl 9-dAX derivatives, respectively.

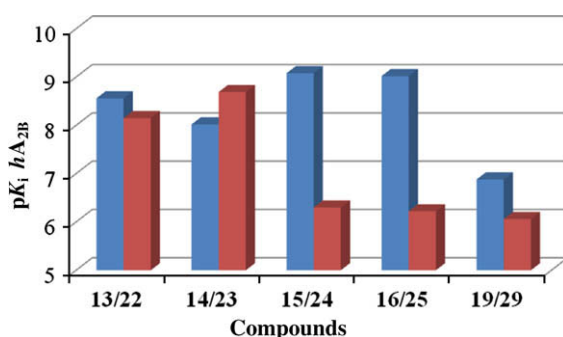


Figure 4. hA_{2B} pK_i comparison of 1,3-dimethyl- and 1,3-dipropyl-8-N-substituted benzyloxycarbonylamino-9-dAXs, represented in blue and red bars, respectively.

4.2. Water solubility and partition coefficients

Despite their excellent affinity and selectivity profiles, 8-N-substituted 9-dAXs generally exhibited low water solubility and high partition coefficients that have strongly limited their development as *in vivo* bioactive agents.^{14–16} To verify an eventual improvement of these key physicochemical properties in the present series of 9-dAX carbamates, two reference compounds, that is, **15** and **22**, have been assessed. Their octanol–water partition coefficients calculated by the Biolum (v.1.5)²⁷ and the ACD/Labs (v. 11.0)²⁸ were 2.25 and 4.57, and 2.01 and 4.46, respectively. Water solubility, measured by the same method previously used for different 9-dAX derivatives,¹⁶ were 21.5 ± 4 and 27 ± 3 $\mu\text{g/ml}$ for compound **15** and **22**, respectively.

4.3. Molecular modeling

To help elucidate the hypothetical different binding modes of 8-N-substituted benzyloxycarbonylamino- and 8-N-substituted phenoxyacetamido-9-dAXs the main structural and molecular properties of these two classes of AR ligands were evaluated by a computational study on reference molecules **A** and **B** (Chart 3).

Using molecules **A** and **B** as a query, a substructure search of the Cambridge Crystallographic Data Centre (CCDC)²⁹ was made. It

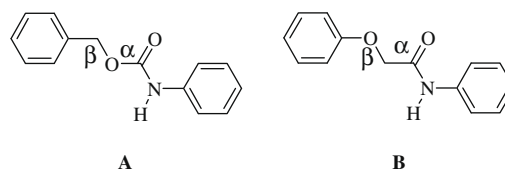


Chart 3. 8-N-Substituted benzyloxycarbonylamino- and 8-N-substituted phenoxyacetamido-9-dAX reference molecules **A** and **B**, respectively.

came out that while crystal structures related to carbamate **A** normally adopted extended conformations, those associated to oxyacetamide **B** assumed generally a folded rather than a linear conformation and this was likely due to the occurrence of an intramolecular HB involving the phenol oxygen and the amidic hydrogen atoms. To obtain a more complete picture of the conformational space accessible to both **A** and **B** molecules, a conformational analysis was run in an apolar implicit solvent (CHCl_3) which supposedly better simulates the inner binding sites and environment of GPCR transmembranes. The variation of molecular energy at the change of α and β angles (Chart 3) confirmed the preference for extended and folded conformations of molecules **A** and **B**, respectively (data not shown).

To complete our computational investigation, atomic charges and molecular electrostatic potentials (MEPs)³⁰ of molecules **A** and **B** were also calculated (data not shown). As expected, the two reference molecules showed different values and distributions of partial charges which might strongly influence the HB formation and the local and global lipophilicity. Indeed, a GRID³¹ analysis performed using the DRY lipophilic probe and the OH polar probe (data not shown) fully supported such a hypothesis. Taken together, our computational data suggested that the two examined molecules might engage significantly diverse HB, polar and hydrophobic interactions, likely arising from their different binding conformations, despite the apparently high structural similarity of the two molecular fragments linking the two phenyl groups.

The same considerations may apply to the carbamic and oxyacetamido 9-dAXs analyzed herein. Indeed, the two different linkers and, more so, the 1,3-dialkyl groups of dAX moieties, might bind in completely diverse modes and regions to the ARs binding sites. Consequently, SAR and SSR relationships of the two classes of 9-dAXs resulted as being completely different.

5. Conclusions

1,3-Dialkyl-8-N-substituted benzyloxycarbonylamino-9-dAXs, represent a novel class of AR ligands endowed with nanomolar affinities at the hA_{2B} , hA_1 and hA_{2A} AR subtypes. Unfortunately, no ligand exhibited an acceptably high selectivity versus the hA_{2B} AR and this strongly limits their therapeutic potential as antiasthmatic agents.

Partition and solubility data assessed for two 1,3-dialkyl-8-N-substituted benzyloxycarbonylamino-9-dAXs might suggest a more favourable *in vivo* activity compared to the corresponding 8-N-substituted phenoxyacetamido analogues.¹⁶

1,3-Dimethyl-*N*-3'-thienyl carbamate **15**, which resulted the most potent ligand at hA_{2B} , with a good selectivity versus hA_3 but poor selectivities versus hA_{2A} and hA_1 , might be taken as a lead for further structural modifications aimed at improving its selectivity profile versus hA_{2B} . Similarly, structural variations on 1,3-dipropyl-*N*-*p*-F-phenyl carbamate **23**, the most potent ligand at the hA_1 in the whole series, might be carried out to ameliorate the selectivity versus this AR subtype. These important goals might be better attained taking into account our computational findings suggesting likely different binding modes of 1,3-dialkyl-8-N-

substituted benzyloxycarbonylamino- and 8-N-substituted phenoxacetamido-9-dAXs at the four AR subtypes.

6. Experimental

6.1. Chemistry

All chemicals used were of reagent grade and were obtained from Aldrich Chemical Co. and used without further purification. When necessary, solvents were dried by standard techniques and distilled. All air-sensitive reactions were carried out under argon. Flash chromatography was performed on silica gel (Merck 60, 230–240 mesh) and analytical TLC on pre-coated silica gel plates (Merck 60 F₂₅₄, 0.25 mm). Melting points (uncorrected) were measured in a glass capillary tube on a Stuart Scientific electro thermal apparatus SMP3. Infrared spectra were recorded in a Perkin–Elmer 1640 FTIR spectrophotometer. ¹H NMR spectra were recorded in a Bruker AMX 300 spectrometer at 300 MHz, using TMS as internal standard (chemical shifts in δ values, *J* in hertz). Mass spectra were recorded on a Hewlett-Packard HP5988A or a Micromass Autospec spectrometers or a Electrospray interface Ion Trap Mass spectrometer. (1100 series LC/MSD Trap System Agilent, Palo Alto, Ca). Microanalyses were performed in a FISIONS EA 1108 Elemental Analyser at the University of Santiago Microanalysis Service; all results shown are within $\pm 0.4\%$ of the theoretical values.

Aryl isocyanates needed for the preparation of target carbamates **13–18**, **21** and **23–26** were either commercially available or recently obtained by standard methods, from the corresponding amines,³² or, when amines were not commercially available, from the appropriate carboxylic acids.³³

6.1.1. General procedure for the condensation between benzaldehydes **9** and 5-nitro-6-methyluracils **8**. Preparation of 1,3-dialkyl-6-styryluracil derivatives **10a, b, d**

A solution of the suitable 1,3-dialkyl-6-methyl-5-nitropyrimidine-2,4-(1*H*,3*H*)-dione **8a, b, c** (8 mmol), the appropriate benzaldehyde (8 mmol), piperidine (12 mmol) and molecular sieves of 3 Å in dry dioxane (50 mL) was refluxed for 5–47 h, under argon atmosphere. The resulting solution was concentrated under vacuum, and the residue was dissolved in EtOAc and successively washed with 10% HCl and brine, dried (Na₂SO₄), and the solvent was evaporated under reduced pressure. The solid residue was purified by CC or recrystallized.

6.1.1.1. 4-[(E)-2-(1,2,3,6-Tetrahydro-1,3-dimethyl-5-nitro-2,6-dioxypyrimidin-4-yl)vinyl]benzoic acid (10a). Yield 70%, mp: 254–256 °C (EtOH). ¹H NMR (DMSO-*d*₆): 13.15 (br s, 1H, CO₂H), 7.99 (d, *J* = 8.2, 2H, C₆H₄), 7.78 (d, *J* = 8.2, 2H, C₆H₄), 7.36 (d, *J* = 16.5, 1H, HC=CH), 7.06 (d, *J* = 16.5, 1H, HC=CH), 3.39 (s, 3H, NCH₃), 3.26 (s, 3H, NCH₃). MS (EI) (*m/z*, %): 331 (M⁺, 0.5), 267 (100).

6.1.1.2. 4-[(E)-2-(1,2,3,6-Tetrahydro-5-nitro-2,6-dioxo-1,3-dipropylpyrimidin-4-yl)vinyl]benzoic acid (10b). CC (hexane/EtOAc, 55:45), yield 80%, mp: 178–180 °C. ¹H NMR (DMSO-*d*₆): 11.14 (br s, 1H, CO₂H), 7.99 (d, *J* = 8.3, 2H, C₆H₄), 7.78 (d, *J* = 8.3, 2H, C₆H₄), 7.37 (d, *J* = 16.4, 1H, HC=CH), 7.10 (d, *J* = 16.4, 1H, HC=CH), 3.87–3.80 (m, 4H, 2 × NCH₂), 1.67–1.55 (m, 4H, 2 × CH₂), 0.91–0.80 (m, 6H, 2 × CH₃). MS (CI) (*m/z*, %): 388 [(M+1)⁺, 100].

6.1.1.3. 6-[(E)-4-(Hydroxymethyl)styryl]-5-nitro-1,3-dipropylpyrimidine-2,4-(1*H*,3*H*)-dione (10c). CC (hexane/EtOAc, 1:1), yield 40%, mp: 134–136 °C. ¹H NMR (CDCl₃): 7.35–7.24 (m, 4H, C₆H₄), 6.92 (d, *J* = 16.3, 1H, HC=CH), 6.55 (d, *J* = 16.3, 1H, HC=CH), 4.58 (s, 2H, OCH₂), 3.86–3.70 (m, 4H, 2 × NCH₂), 3.41 (br s, 1H, OH), 1.66–1.52 (m, 4H, 2 × CH₂), 0.86–0.80 (m, 6H, 2 × CH₃). MS (EI) (*m/z*, %): 373 (M⁺, 11), 309 (100).

6.1.1.4. 4-[(E)-2-(1,2,3,6-Tetrahydro-3-Methyl-5-nitro-2,6-dioxo-1-propylpyrimidin-4-yl)-vinyl]-benzoic acid (10d). CC (CHCl₃/MeOH, 9:1), yield 65%, mp: 188–190 °C (dec). ¹H NMR (DMSO-*d*₆): 10.50 (br s, 1H, CO₂H), 7.88 (d, *J* = 8.3, 2H, C₆H₄), 7.57 (d, *J* = 8.3, 2H, C₆H₄), 7.16 (d, *J* = 16.2, 1H, HC=CH), 6.98 (d, *J* = 16.2, 1H, HC=CH), 3.80 (t, *J* = 7.2, 2H, NCH₂), 3.35 (s, 3H, NCH₃), 1.68–1.59 (m, 2H, CH₂), 0.87 (t, 3H, *J* = 7.4, CH₃). MS (ESI) (*m/z*, %): 358 [(M–1)[–], 100].

6.1.2. General procedure for the reductive ring closure of 5-nitro-6-styryluracils **10a–d** to **11a–d**

To a solution of the appropriate 5-nitro-6-styryluracil derivative **10a–d** (5 mmol) in formic acid (40 mL) was slowly added sodium dithionite (11.5 mmol) and the mixture was refluxed overnight. The resulting suspension was cooled to room temperature and poured into water. The precipitate was collected by filtration, washed with water and dried under vacuum to yield the expected compounds **11a–d**.

6.1.2.1. 4-(2,3,4,5-Tetrahydro-1,3-dimethyl-2,4-dioxo-1*H*-pyrrolo[3,2-*d*]pyrimidin-6-yl)benzoic acid (11a). Yield 80%, mp: >300 °C (H₂O). ¹H NMR (DMSO-*d*₆): 12.93 (br s, 1H), 12.52 (br s, 1H), 8.04–7.93 (m, 4H, C₆H₄), 6.78 (s, 1H, 7-H), 3.33 (s, 3H, NCH₃), 3.17 (s, 3H, NCH₃). MS (EI) (*m/z*, %): 299 (M⁺, 100).

6.1.2.2. 4-(2,3,4,5-Tetrahydro-2,4-dioxo-1,3-dipropyl-1*H*-pyrrolo[3,2-*d*]pyrimidin-6-yl)benzoic acid (11b). Yield 90%, mp: 340–345 °C (dec) (MeOH/Et₂O). ¹H NMR (DMSO-*d*₆): 12.88 (br s, 1H), 12.42 (br s, 1H), 7.92–7.82 (m, 4H, C₆H₄), 6.75 (s, 1H, 7-H), 3.73 (m, 4H, 2 × NCH₂), 1.56–1.43 (m, 4H, 2 × CH₂), 0.78–0.73 (m, 6H, 2 × CH₃). MS (CI) (*m/z*, %): 356 [(M+1)⁺, 100].

6.1.2.3. 4-(2,3,4,5-Tetrahydro-2,4-dioxo-1-methyl-3-propyl-1*H*-pyrrolo[3,2-*d*]pyrimidin-6-yl)benzoic acid (11d). Yield 18%, mp: >300 °C (MeOH/Et₂O). ¹H NMR (DMSO-*d*₆): 12.92 (br s, 1H), 12.55 (br s, 1H), 8.00–7.94 (m, 4H, C₆H₄), 6.85 (s, 1H, 7-H), 3.83 (t, *J* = 7.4, 2H, NCH₂), 1.61–1.52 (m, 2H, CH₂), 0.87 t, *J* = 7.4, 3H, CH₃). MS (ESI) (*m/z*, %): 326 [(M–1)[–], 100].

6.1.2.4. [4-(2,3,4,5-Tetrahydro-2,4-dioxo-1,3-dipropyl-1*H*-pyrrolo[3,2-*d*]pyrimidin-6-yl)phenyl]methyl formate (11c). CC (hexane/EtOAc, 7:3), yield 17%, mp: 229–231 °C (EtOAc). ¹H NMR (CDCl₃): 11.73 (br s, 1H, NH), 8.16 (s, 1H, CO₂H), 7.88 (d, *J* = 8.2, 2H, C₆H₄), 7.44 (d, *J* = 8.2, 2H, C₆H₄), 6.27 (s, 1H, 7-H), 5.24 (s, 2H, OCH₂), 4.06–3.91 (m, 4H, 2 × NCH₂), 1.82 (sext, *J* = 7.4, 2H, CH₂), 1.67 (sext, *J* = 7.4, 2H, CH₂), 1.02 (t, *J* = 7.4, 3H, CH₃), 0.87 (t, *J* = 7.4, 3H, CH₃). MS (EI) (*m/z*, %): 369 (M⁺, 84), 285 (100).

6.1.3. General procedure for the reduction of compounds **11a, b, d**

The carboxylic acid **11** (4 mmol) was suspended in anhydrous THF (25 mL) and the mixture was cooled to 0 °C. 1 M BH₃·THF in THF (10 mL) was added, and the resulting suspension was stirred at rt between 6 and 24 h. MeOH was cautiously added to the cooled mixture and the solvents were evaporated under reduced pressure. The solid residue was dissolved in EtOAc and the solution was successively washed with 10% NaOH and H₂O. The organic layer was dried (Na₂SO₄), filtered and the solvent was evaporated to give the corresponding hydroxymethyl derivatives of the pyrrolo[3,2-*d*]pyrimidine-2,4-(3*H*,5*H*)-dione, **12a, b, d**.

6.1.3.1. 6-[4-(Hydroxymethyl)phenyl]-1,3-dimethyl-1*H*-pyrrolo[3,2-*d*]pyrimidine-2,4-(3*H*,5*H*)-dione (12a). Yield 40%, mp: 266–268 °C (MeOH/Et₂O). ¹H NMR (DMSO-*d*₆): 12.34 (br s, 1H, NH), 7.84 (d, *J* = 8.1, 2H, C₆H₄), 7.34 (d, *J* = 8.1, 2H, C₆H₄), 6.67 (s,

1H, 7-H), 5.21 (t, $J = 5.6$, 1H, OH), 4.48 (d, $J = 5.6$, 2H, OCH₂), 3.39 (s, 3H, NCH₃), 3.23 (s, 3H, NCH₃). MS (EI) (m/z , %): 285 (M^+ , 100).

6.1.3.2. 6-[4-(Hydroxymethyl)phenyl]-1,3-dipropyl-1H-pyrrolo[3,2-d]pyrimidine-2,4(3H,5H)-dione (12b). Yield 90%, mp: 282–285 °C (dec) (MeOH/Et₂O). ¹H NMR (DMSO-*d*₆): 12.17 (br s, 1H), 7.72 (d, $J = 8.0$, 2H, C₆H₄), 7.20 (d, $J = 8.0$, 2H, C₆H₄), 6.57 (s, 1H, 7-H), 5.08 (t, $J = 5.6$, 1H, OH), 4.36 (d, $J = 5.6$, 2H, OCH₂), 3.73–3.67 (m, 4H, 2 × NCH₂), 1.54–1.40 (m, 4H, 2 × CH₂), 0.78–0.67 (m, 6H, 2 × CH₃). MS (CI) (m/z , %): 342 [($M+1$)⁺, 100].

6.1.3.3. 6-[4-(Hydroxymethyl)phenyl]-1-methyl-3-propyl-1H-pyrrolo[3,2-d]pyrimidine-2,4(3H,5H)-dione (12d). Yield 75%, mp: 200–202 °C (dec) (MeOH/Et₂O). ¹H NMR (DMSO-*d*₆): 12.17 (br s, 1H), 7.85 (d, $J = 8.1$, 2H, C₆H₄), 7.35 (d, $J = 8.1$, 2H, C₆H₄), 6.68 (s, 1H, 7-H), 5.20 (t, $J = 5.3$, 1H, OH), 4.50 (d, $J = 5.3$, 2H, OCH₂), 3.84 (t, $J = 7.4$, NCH₂), 3.59 (s, 3H, NCH₃), 1.48–1.38 (m, 2H, CH₂), 0.86 (t, $J = 7.4$, 3H, CH₃). MS (ESI) (m/z , %): 312 [($M-1$)⁺, 100].

6.1.4. General procedures for the preparation of carbamates 13–32 from the appropriate hydroxymethyl derivatives 12a, b d (see Scheme 1)

Method A. The aryl isocyanate (0.42 mol) was added to a freshly prepared solution of the hydroxymethyl derivative **12a** or **12b** (0.35 mol) in dry DMF (5 mL), under Ar atmosphere and at rt, and the mixture was thereafter heated at 115 °C until the disappearance of the starting material was observed (TLC, CH₂Cl₂/MeOH, 5–7 h). The reaction mixture was then poured into H₂O (20 mL) and extracted with EtOAc (3 × 25 mL). The combined extracts were washed with H₂O, and dried (Na₂SO₄). The solvent was evaporated under reduced pressure and the residue was recrystallized from MeOH.

Method B. The hydroxymethyl derivative **12a**, **b**, **d** (0.31 mol) in dry dioxane (6 mL) was added to a freshly prepared solution of the isocyanate (0.77 mol) in dry dioxane or toluene (6 mL) under Ar atmosphere and the mixture was stirred while heating to reflux. Progress of the reactions was monitored by TLC, and when no more starting material was detected, the solvent was evaporated under reduced pressure and the residue was purified by CC (CH₂Cl₂/MeOH) or recrystallized from mixtures of CH₂Cl₂/MeOH.

Method C. A solution of the hydroxymethyl derivative **12a**, **b**, **d** (0.29 mol) in dry pyridine (1 mL) was added to the solution of CDI (0.29 mol) in dry pyridine (0.5 mL), at 0 °C and under Ar atmosphere. The reaction mixture was stirred 2 h at this temperature, and it was thereafter allowed to reach rt and stirred for a further 2 h. The corresponding amine (0.29 mol) was then slowly added while stirring and the precipitate formed was collected by filtration and washed with water.

6.1.4.1. [4-(2,3,4,5-Tetrahydro-1,3-dimethyl-2,4-dioxo-1H-pyrrolo[3,2-d]pyrimidin-6-yl)phenyl]methyl phenylcarbamate (13). **Method A.** Yield 40%, mp: 249–251 °C. ¹H NMR (DMSO-*d*₆): 12.50 (s, 1H, NH), 9.85 (s, 1H, NH), 8.00 (d, $J = 8.2$, 2H, arom.), 7.56–7.51 (m, 4H, arom.), 7.35–7.32 (m, 2H, arom.), 7.09–7.02 (m, 1H, arom.), 6.81 (s, 1H, 7-H), 5.23 (s, 2H, OCH₂), 3.49 (s, 3H, NCH₃), 3.32 (s, 3H, NCH₃). MS (EI) (m/z , %): 404 (M^+ , 8), 268 (100). Anal. Calcd for C₂₂H₂₀N₄O₄: C, 65.34; H, 4.96; N, 13.85. Found: C, 65.01; H, 5.31; N, 14.11.

6.1.4.2. [4-(2,3,4,5-Tetrahydro-1,3-dimethyl-2,4-dioxo-1H-pyrrolo[3,2-d]pyrimidin-6-yl)phenyl]methyl 4-fluorophenylcarbamate (14). **Method A.** Yield 43%, mp 280–282 °C. ¹H NMR (DMSO-*d*₆): 12.52 (s, 1H, NH), 9.91 (s, 1H, NH), 8.00 (d, 2H, $J = 8.2$, arom.), 7.56–7.51 (m, 4H, arom.), 7.35–7.32 (m, 2H, arom.), 6.83 (s, 1H, 7-H), 5.24 (s, 2H, OCH₂), 3.50 (s, 3H, NCH₃), 3.33 (s, 3H, NCH₃). MS (EI)

(m/z , %): 422 (M^+ , 0.2), 63 (100). Anal. Calcd for C₂₂H₁₉FN₄O₄: C, 62.55; H, 4.53; N, 13.26. Found: C, 62.88; H, 4.71; N, 13.42.

6.1.4.3. [4-(2,3,4,5-Tetrahydro-1,3-dimethyl-2,4-dioxo-1H-pyrrolo[3,2-d]pyrimidin-6-yl)phenyl]methyl thiophen-3-ylcarbamate (15). **Method B.** CC (CH₂Cl₂/MeOH, 97:3), yield 20%, mp: 279–281 °C (MeOH). ¹H NMR (DMSO-*d*₆): 12.43 (s, 1H, NH), 10.06 (s, 1H, NH), 7.92 (d, $J = 8.3$, 2H, C₆H₄), 7.45 (d, $J = 8.3$, 2H, C₆H₄), 7.42–7.40 (m, 1H, C₄H₃S), 7.21–7.19 (m, 1H, C₄H₃S), 6.99 (d, $J = 5.1$, 1H, C₄H₃S), 6.74 (s, 1H, 7-H), 5.15 (s, 2H, OCH₂), 3.41 (s, 3H, NCH₃), 3.25 (s, 3H, NCH₃). MS (FAB) (m/z , %): 410 (M , 4), 285 (100). Anal. Calcd for C₂₀H₁₈N₄O₄S: C, 58.53; H, 4.42; N, 13.65; S, 7.81. Found: C, 58.71; H, 4.31; N, 13.97; S, 8.08.

6.1.4.4. [4-(2,3,4,5-Tetrahydro-1,3-dimethyl-2,4-dioxo-1H-pyrrolo[3,2-d]pyrimidin-6-yl)phenyl]methyl thiophen-2-ylcarbamate (16). **Method B.** CC (CH₂Cl₂/MeOH, 95:5), yield 31%, mp: 286–288 °C (MeOH). ¹H NMR (DMSO-*d*₆): 12.36 (s, 1H, NH), 10.67 (s, 1H, NH), 7.86 (d, $J = 8.1$, 2H, C₆H₄), 7.39 (d, $J = 8.1$, 2H, C₆H₄), 6.86–6.84 (m, 1H, C₄H₃S), 6.75–6.71 (m, 1H, C₄H₃S), 6.68 (s, 1H, 7-H), 6.49–6.47 (m, 1H, C₄H₃S), 5.11 (s, 2H, OCH₂), 3.35 (s, 3H, NCH₃), 3.19 (s, 3H, NCH₃). MS (FAB) (m/z , %): 410 (M , 0.7), 285 (100). Anal. Calcd for C₂₀H₁₈N₄O₄S: C, 58.53; H, 4.42; N, 13.65; S, 7.81. Found: C, 58.90; H, 4.21; N, 13.99; S, 7.59.

6.1.4.5. [4-(2,3,4,5-Tetrahydro-1,3-dimethyl-2,4-dioxo-1H-pyrrolo[3,2-d]pyrimidin-6-yl)phenyl]methyl pyridin-2-ylcarbamate (17). **Method B.** Yield 60% mp: 301–303 °C (MeOH). ¹H NMR (DMSO-*d*₆): 12.28 (s, 1H, -NH), 10.13 (s, 1H, NH), 8.10 (d, $J = 5.2$, 1H, C₅H₄N), 7.77 (d, $J = 8.2$, 2H, C₆H₄), 7.69–7.56 (m, 2H, C₅H₄N), 7.32 (d, $J = 8.2$, 2H, C₆H₄), 6.91–6.86 (m, 1H, C₅H₄N), 6.59 (s, 1H, 7-H), 5.03 (s, 2H, OCH₂), 3.26 (s, 3H, NCH₃), 3.10 (s, 3H, NCH₃). MS (FAB) (m/z , %): 406 [($M+1$)⁺, 3], 154 (100). Anal. Calcd for C₂₁H₁₉N₅O₄: C, 62.22; H, 4.72; N, 17.26. Found: C, 62.50; H, 4.75; N, 17.59.

6.1.4.6. [4-(2,3,4,5-Tetrahydro-1,3-dimethyl-2,4-dioxo-1H-pyrrolo[3,2-d]pyrimidin-6-yl)phenyl]methyl furan-2-ylcarbamate (18). **Method B.** CC (CH₂Cl₂/MeOH, 98:2), yield 23%, mp: 278–280 °C (MeOH). ¹H NMR (DMSO-*d*₆): 12.41 (s, 1H, NH), 10.29 (s, 1H, NH), 7.94 (d, $J = 8.1$, 2H, C₆H₄), 7.46 (d, $J = 8.1$, 2H, C₆H₄), 7.33–7.28 (m, 1H, C₄H₃O), 6.75 (s, 1H, 7-H), 6.43–6.40 (m, 1H, C₄H₃O), 6.04–5.98 (m, 1H, C₄H₃O), 5.15 (s, 2H, CH₂), 3.24 (s, 3H, NCH₃), 3.08 (s, 3H, NCH₃). MS (FAB) (m/z , %): 394 [M , 0.7]; 285 (100). Anal. Calcd for C₁₈H₁₄N₄O₅: C, 59.02; H, 3.85; N, 15.29. Found: C, 58.85; H, 4.25; N, 15.59.

6.1.4.7. [4-(2,3,4,5-Tetrahydro-1,3-dimethyl-2,4-dioxo-1H-pyrrolo[3,2-d]pyrimidin-6-yl)phenyl]methyl 4-phenylpiperazine-1-carboxylate (19). **Method C.** Yield 33%, mp: 254–256 °C (EtOAc). ¹H NMR (DMSO-*d*₆): 12.41 (s, 1H, NH), 7.90 (d, $J = 8.2$, 2H, C₆H₄), 7.42 (d, $J = 8.2$, 2H, C₆H₄), 7.37–6.99 (m, 2H, C₆H₅), 6.93 (d, $J = 8.2$, 2H, C₆H₅), 6.81–6.78 (m, 1H, C₆H₅), 6.72 (s, 1H, 7-H), 5.12 (s, 2H, OCH₂), 3.13 (s, 3H, NCH₃), 3.08 (s, 3H, NCH₃). MS (CI) (m/z , %): 85 (100). Anal. Calcd for C₂₅H₂₇N₅O₄: C, 65.95; H, 5.75; N, 14.79. Found: C, 65.88; H, 5.99; N, 15.05.

6.1.4.8. [4-(2,3,4,5-Tetrahydro-1,3-dimethyl-2,4-dioxo-1H-pyrrolo[3,2-d]pyrimidin-6-yl)phenyl]methyl 3,4-dihydroisoquinoline-2(1H)-carboxylate (20). **Method C.** Yield 42%, mp = 225–228 °C (EtOAc). ¹H NMR (DMSO-*d*₆): 12.14 (s, 1H, NH), 7.90 (d, $J = 7.3$, 2H, C₆H₄), 7.42 (d, $J = 7.3$, 2H, C₆H₄), 7.16 (virtual s, 4H, C₉H₁₀N), 6.50 (s, 1H, 7-H), 4.86 (s, 2H, OCH₂), 4.60–4.55 (m, 2H, CH₂), 3.66–3.61 (m, 2H, CH₂), 3.17–3.15 (m, 2H, CH₂), 3.42 (s, 3H, NCH₃), 3.26 (s, 3H, NCH₃). MS (FAB) (m/z , %): 445 [($M+1$)⁺, 9], 444 (M , 1), 270 (100). Anal. Calcd for C₂₅H₂₄N₄O₄: C, 67.55; H, 5.44; N, 12.60. Found: C, 67.88; H, 5.37; N, 12.85.

6.1.4.9. [4-(2,3,4,5-Tetrahydro-1,3-dimethyl-2,4-dioxo-1H-pyrrolo[3,2-d]pyrimidin-6-yl)phenyl]methyl benzylcarbamate (21). Method A. Yield 30%, mp: 233–235 °C. ¹H NMR (DMSO-*d*₆): 12.43 (s, 1H, NH), 7.91 (d, *J* = 8.2, 2H, C₆H₄), 7.41 (d, *J* = 8.2, 2H, C₆H₄), 7.35–7.25 (m, 5H, C₆H₅), 6.75 (s, 1H, 7-H), 5.07 (s, 2H, OCH₂), 4.21 (d, *J* = 5.9, 2H, NCH₂), 3.42 (s, 3H, NCH₃), 3.26 (s, 3H, NCH₃). MS (EI) (*m/z*, %): 418 (M⁺, 47), 268 (99), 63 (100). Anal. Calcd for C₂₃H₂₂N₄O₄: C, 66.02; H, 5.30; N, 13.39. Found: C, 65.88; H, 5.67; N, 13.65.

6.1.4.10. [4-(2,3,4,5-Tetrahydro-2,4-dioxo-1,3-dipropyl-1H-pyrrolo[3,2-d]pyrimidin-6-yl)phenyl]methyl phenylcarbamate (22). Method C. Yield 16%, mp 226–228 °C (MeOH). ¹H NMR (DMSO-*d*₆): 12.35 (s, 1H, NH), 9.74 (s, 1H, NH), 7.91 (dd, *J* = 8.4, 2.9, 2H, arom.), 7.47–7.41 (m, 3H, arom.), 7.28–7.26 (m, 2H, arom.), 6.98 (d, *J* = 7.4, 2H, arom.), 6.75 (s, 1H, 7-H), 5.07 (s, 2H, OCH₂), 3.85 (t, *J* = 7.2, 2 × NCH₂), 1.67 (sext, *J* = 7.1, 2H, CH₂), 1.56 (sext, *J* = 7.3, 2H, CH₂), 0.91 (t, *J* = 7.2, 3H, CH₃), 0.86 (t, *J* = 7.3, 3H, CH₃). MS (FAB) (*m/z*, %): 460 [M, 26]; 324 (100). Anal. Calcd for C₂₆H₂₈N₄O₄: C, 67.81; H, 6.13; N, 12.17. Found: C, 68.18; H, 6.06; N, 12.25.

6.1.4.11. [4-(2,3,4,5-Tetrahydro-2,4-dioxo-1,3-dipropyl-1H-pyrrolo[3,2-d]pyrimidin-6-yl)phenyl]methyl 4-fluorophenylcarbamate (23). Method A. Yield 43%, mp 259–261 °C (EtOAc). ¹H NMR (DMSO-*d*₆): 12.35 (s, 1H, NH), 9.79 (s, 1H, NH), 8.26 (virtual s, 2H, C₆H₄F), 7.90 (d, *J* = 8.2, 2H, C₆H₄), 7.84 (d, *J* = 7.8, 2H, C₆H₄), 7.08 (t, *J* = 7.8, 2H, C₆H₄F), 6.72 (s, 1H, 7-H), 5.14 (s, 2H, OCH₂), 3.85 (t, *J* = 7.4 Hz, 2H, NCH₂), 3.35 (t, *J* = 7.4 Hz, 2H, NCH₂), 1.72–1.65 (m, 2H, CH₂), 1.59–1.52 (m, 2H, CH₂), 0.90 (t, *J* = 7.3, 3H, CH₃), 0.83 (t, *J* = 7.3, 3H, CH₃). MS (FAB) (*m/z*, %): 478 (M, 23); 341 (100). Anal. Calcd for C₂₆H₂₇FN₄O₄: C, 65.26; H, 5.69; N, 11.71. Found: C, 65.58; H, 5.97; N, 11.65.

6.1.4.12. [4-(2,3,4,5-Tetrahydro-2,4-dioxo-1,3-dipropyl-1H-pyrrolo[3,2-d]pyrimidin-6-yl)phenyl]methyl thiophen-3-ylcarbamate (24). Method B. Yield 75%, mp >320 °C (toluene). ¹H NMR (DMSO-*d*₆): 12.34 (s, 1H, NH), 10.08 (s, 1H, NH), 7.89 (d, *J* = 8.0, 2H, C₆H₄), 7.42–7.36 (m, 3H, C₆H₄ + C₄H₃S), 7.16 (s, 1H, C₄H₃S), 6.98 (d, *J* = 4.6, 1H, C₄H₃S), 6.73 (s, 1H, 7-H), 5.11 (s, 2H, OCH₂), 3.81 (t, *J* = 6.9, 4H, 2 × NCH₂), 1.70–1.47 (m, 4H, 2 × CH₂), 0.86 (t, *J* = 7.2, 3H, CH₃), 0.81 (t, *J* = 7.3, 3H, CH₃). MS (FAB) (*m/z*, %): 467 [(M+1)⁺, 3], 177 (100). Anal. Calcd for C₂₄H₂₆N₄O₄S: C, 61.79; H, 5.62; N, 12.01, S, 6.87. Found: C, 61.92; H, 5.46; N, 12.45, S, 7.12.

6.1.4.13. [4-(2,3,4,5-Tetrahydro-2,4-dioxo-1,3-dipropyl-1H-pyrrolo[3,2-d]pyrimidin-6-yl)phenyl]methyl thiophen-2-ylcarbamate (25). Method B. Yield 90%, mp 245–247 °C (toluene). ¹H NMR (DMSO-*d*₆): 12.26 (s, 1H, NH), 10.68 (s, 1H, NH), 7.82 (d, *J* = 8.1, 2H, C₆H₄), 7.34 (d, *J* = 8.1, 2H, C₆H₄), 8.89–6.80 (m, 1H, C₄H₃S), 6.79–6.77 (m, 2H, C₄H₃S), 6.46 (s, 1H, 7-H), 5.05 (s, 2H, OCH₂), 3.73 (t, *J* = 6.9, 4H, 2 × NCH₂), 1.61–1.40 (m, 4H, 2 × CH₂), 0.79 (t, *J* = 7.2, 3H, CH₃), 0.74 (t, *J* = 7.2, 3H, CH₃). MS (FAB) (*m/z*, %): 467 [(M+1)⁺, 3], 154 (100). Anal. Calcd for C₂₄H₂₆N₄O₄S: C, 61.79; H, 5.62; N, 12.01; S, 6.87. Found: C, 61.99; H, 5.36; N, 11.85; S, 6.77.

6.1.4.14. [4-(2,3,4,5-Tetrahydro-2,4-dioxo-1,3-dipropyl-1H-pyrrolo[3,2-d]pyrimidin-6-yl)phenyl]methyl pyrazin-2-ylcarbamate (26). Method B. CC (CH₂Cl₂/MeOH, 95:5), yield 19%, mp 268–270 °C (Et₂O). ¹H NMR (DMSO-*d*₆): 12.38 (s, 1H, NH), 10.65 (s, 1H, NH), 9.09 (s, 1H, C₆H₃N₂), 8.34–8.29 (m, 2H, C₆H₃N₂), 7.95 (d, *J* = 8.1, 2H, C₆H₄), 7.48 (d, *J* = 8.1, 2H, C₆H₄), 6.77 (s, 1H, 7-H), 5.22 (s, 2H, OCH₂), 3.87–3.82 (m, 4H, 2 × NCH₂), 1.71–1.50 (m, 4H, 2 × CH₂), 0.92–0.82 (m, 6H, 2 × CH₃). MS (FAB) (*m/z*, %): 463 [(M+1)⁺, 4], 154 (100). Anal. Calcd for C₂₄H₂₆N₆O₄: C, 62.33; H, 5.67; N, 18.17. Found: C, 62.59; H, 5.78; N, 18.45.

6.1.4.15. [4-(2,3,4,5-Tetrahydro-2,4-dioxo-1,3-dipropyl-1H-pyrrolo[3,2-d]pyrimidin-6-yl)phenyl]methyl isoxazol-2-ylcarbamate (27). Method C. Yield 41%, mp 169–171 °C (EtOAc). ¹H NMR (DMSO-*d*₆): 12.40 (s, 1H, NH), 8.30 (s, 1H, NH), 7.95 (d, *J* = 8.0, 2H, C₆H₄), 7.60 (d, *J* = 8.0, 2H, C₆H₄), 6.76 (s, 1H, 7-H), 5.77–5.70 (m, 1H, C₃H₂NO), 5.55–5.42 (m, 1H, C₃H₂NO), 5.41 (s, 2H, OCH₂), 3.86–3.75 (m, 4H, 2 × NCH₂), 1.82–1.63 (m, 4H, 2 × CH₂), 0.99–0.88 (m, 6H, 2 × CH₃). MS (FAB) (*m/z*, %): 324 (100). Anal. Calcd for C₂₃H₂₅N₅O₅: 61.19; H, 5.58; N, 15.51. Found: C, 61.59; H, 5.88; N, 15.85.

6.1.4.16. [4-(2,3,4,5-Tetrahydro-2,4-dioxo-1,3-dipropyl-1H-pyrrolo[3,2-d]pyrimidin-6-yl)phenyl]methyl 1H-pyrazol-3-ylcarbamate (28). Method C. Yield 60%, mp 211–213 °C (EtOAc). ¹H NMR (DMSO-*d*₆): 12.39 (s, 1H, NH), 8.03–7.93 (m, 4H, C₆H₄ + NH + C₃H₂N₂), 7.49 (d, *J* = 7.9, 2H, C₆H₄), 6.78 (s, 1H, 7-H), 5.85 (s, 1H, NH), 5.51 (s, 1H, C₃H₂N₂), 5.33 (s, 2H, OCH₂), 3.89–3.83 (m, 4H, 2 × NCH₂), 1.70–1.52 (m, 4H, 2 × CH₂), 0.91 (t, *J* = 7.3, 3H, CH₃), 0.86 (t, *J* = 7.3, 3H, CH₃). MS (FAB) (*m/z*, %): 450 (M, 3). Anal. Calcd for C₂₃H₂₆N₆O₄: C, 61.32; H, 5.82; N, 18.66. Found: C, 61.38; H, 5.72; N, 18.27.

6.1.4.17. [4-(2,3,4,5-Tetrahydro-2,4-dioxo-1,3-dipropyl-1H-pyrrolo[3,2-d]pyrimidin-6-yl)phenyl]methyl 4-phenylpiperazine-1-carboxylate (29). Method C. Yield 33%, mp 240–242 °C (EtOAc). ¹H NMR (DMSO-*d*₆): 12.36 (s, 1H, NH), 7.90 (d, *J* = 8.2, 2H, C₆H₄), 7.42 (d, *J* = 8.2, 2H, C₆H₄), 7.24–7.19 (m, 2H, C₆H₅), 6.94 (d, *J* = 8.2, C₆H₅), 6.80 (t, *J* = 7.2, C₆H₅), 6.75 (s, 1H, 7-H), 5.12 (s, 2H, OCH₂), 3.89–3.84 (m, 4H, 2 × NCH₂), 3.60–3.51 (m, 4H, 2 × NCH₂), 3.13–3.10 (m, 4H, 2 × NCH₂), 1.68 (sext, *J* = 7.3, 2H, CH₂), 1.57 (sext, *J* = 7.3, 2H, CH₂), 0.91 (t, *J* = 7.2, 3H, CH₃), 0.86 (t, *J* = 7.2, 3H, CH₃). MS (FAB) (*m/z*, %): 530 [(M+1)⁺, 5]. Anal. Calcd for C₃₀H₃₅N₅O₄: C, 68.03; H, 6.66; N, 13.22. Found: C, 68.25; H, 6.98; N, 13.11.

6.1.4.18. [4-(2,3,4,5-Tetrahydro-2,4-dioxo-1,3-dipropyl-1H-pyrrolo[3,2-d]pyrimidin-6-yl)phenyl]methyl 4-(3-chlorophenyl)piperazine-1-carboxylate (30). Method C. Yield 15%, mp 188–190 °C (EtOAc). ¹H NMR (DMSO-*d*₆): 12.36 (s, 1H, NH), 7.91 (d, *J* = 8.1, 2H, C₆H₄), 7.42 (d, *J* = 8.1, 2H, C₆H₄), 7.32–7.25 (m, 1H, C₆H₄Cl), 6.95–6.88 (m, 2H, C₆H₄Cl), 6.82–6.73 (m, 2H, C₆H₄Cl + 7-H), 5.11 (s, 2H, OCH₂), 3.88–3.81 (m, 4H, 2 × NCH₂), 3.52–3.45 (m, 4H, 2 × NCH₂), 3.41–3.30 (m, 4H, 2 × NCH₂), 1.69–1.54 (m, 4H, 2 × CH₂), 0.93–0.83 (m, 6H, 2 × CH₃). MS-FAB (*m/z*, %): 564 [(M+1)⁺, 6]. Anal. Calcd for C₃₀H₃₄ClN₅O₄: C, 63.88; H, 6.08; N, 12.42. Found: C, 63.65; H, 5.95; N, 12.64.

6.1.4.19. [4-(2,3,4,5-Tetrahydro-2,4-dioxo-1,3-dipropyl-1H-pyrrolo[3,2-d]pyrimidin-6-yl)phenyl]methyl 4-(4-fluorophenyl)piperazine-1-carboxylate (31). Method C. Yield 24%, mp 225–227 °C (EtOAc). ¹H NMR (DMSO-*d*₆): 12.31 (s, 1H, NH), 7.84 (d, *J* = 8.2, 2H, C₆H₄), 7.35 (d, *J* = 8.2, 2H, C₆H₄), 7.01–6.89 (m, 4H, C₆H₄F), 6.68 (s, 1H, 7-H), 5.04 (s, 2H, OCH₂), 3.81–3.76 (m, 4H, 2 × NCH₂), 3.60–3.43 (m, 4H, 2 × NCH₂), 2.98–2.92 (m, 4H, 2 × NCH₂), 1.61–1.47 (m, 4H, 2 × CH₂), 0.86–0.76 (m, 6H, 2 × CH₃). MS (FAB) (*m/z*, %): 342 (100). Anal. Calcd for C₃₀H₃₄FN₅O₄: C, 65.80; H, 6.26; N, 12.79. Found: C, 66.13; H, 6.49; N, 12.98.

6.1.4.20. [4-(2,3,4,5-Tetrahydro-2,4-dioxo-1-methyl-3-propyl-1H-pyrrolo[3,2-d]pyrimidin-6-yl)phenyl]methyl phenylcarbamate (32). Method B. Yield 25%, mp 273–275 °C (MeOH). ¹H NMR (DMSO-*d*₆): 12.21 (s, 1H, NH), 9.76 (s, 1H, NH), 7.90 (d, *J* = 7.15, 2H, arom.), 7.48–7.40 (m, 4H, arom.), 7.28–7.24 (m, 2H, arom.), 6.98–6.96 (m, 1H, arom.), 6.73 (s, 1H, 7-H), 5.15 (s, 2H, OCH₂), 3.85 (t, *J* = 7.2, 2H, NCH₂), 3.4 (s, 3H, NCH₃), 1.58–1.50 (m, 2H, CH₂), 0.91 (t, *J* = 7.2, 3H, CH₃), 0.86 (t, *J* = 7.3, 3H, CH₃). MS (ESI) (*m/z*, %): 431 [(M–1)[–], 100]. Anal. Calcd for C₂₄H₂₄N₄O₄: C, 66.65; H, 5.59; N, 12.96. Found: C, 66.43; H, 5.71; N, 12.80.

6.2. Water solubility assay

The compound was dissolved in DMSO at a concentration of 1 mg/ml. This solution was added in portion, (2 μ l at a time) to 1 ml of a 50 mM Tris/HCl pH 7.4 buffer solution at room temperature. Typically a total of 14 additions were made so that the final volume of DMSO was well below 5%. The appearance of the precipitate was detected by an absorbance increase, due to light scattering by particulate material, in a dedicate diode array UV spectrometer (GE Healthcare). Increased UV absorbance was measured in the 600–820 nm range. In its simplest implementation, the precipitation point (i.e., the upper aqueous solubility limit), was calculate from a bilinear curve fit in a plot of the absorbance (y axis) versus μ l of DMSO (x axis). The results reported in Section 4.2 are the means \pm SEM of two independent assays.

6.3. Molecular modeling

Reference molecules **A** and **B** (Chart 3) were built starting from the SENFOH and FAXYN crystal structures [CCDC].²⁹ Geometrical optimization and conformational analyses were performed with MACROMODEL,³⁴ using the force field OPLS 2001.^{35,36} The molecular structures were minimized using the conjugated gradient algorithm setting the number of iterations equal to 1000 and the value of convergence equal to 0.025 Å.

The conformational analyses were performed setting a step equal to 15° for both α and β dihedral angles. 576 conformations were obtained and single point energy calculations were performed. Contour maps were generated by using an in-house script written in MatLab.³⁷ Charge calculations were made by means of a quantum mechanical method with the PM3 Hamiltonian available in MOPAC 6.0.³⁸ The molecular electrostatic potential (MEP) was calculated with VEGA-ZZ setting the point density and the probe radius equal to 2500 and 1.4 Å, respectively.³⁰ By using standard options, molecular interaction fields (MIFs) were calculated within GRID³¹ using DRY and OH and probes.

6.4. Biochemistry and pharmacology

6.4.1. Radioligand binding assays

Radioligand binding competition assays were performed in vitro using A₁, A_{2A}, A_{2B} and A₃ human receptors expressed in transfected CHO (hA₁), HeLa (hA_{2A} and hA₃) and HEK-293 (hA_{2B}) cells as previously described.¹⁶ Briefly:

6.4.1.1. Human A₁ receptors. Adenosine A₁ receptor competition binding experiments were carried out in membranes from CHO-A₁ cells (Euroscreen, Gosselies, Belgium) labeled with 2 nM [³H]DPCPX. Non-specific binding was determined in the presence of 10 μ M (R)-PIA. The reaction mixture was incubated at 25 °C for 60 min.

6.4.1.2. Human A_{2A} receptors. Adenosine A_{2A} receptor competition binding experiments were carried out in membranes from HeLa-A_{2A} cells labeled with 3 nM [³H]ZM241385. Non-specific binding was determined in the presence of 50 μ M NECA. The reaction mixture was incubated at 25 °C for 30 min.

6.4.1.3. Human A_{2B} receptors. Adenosine A_{2B} receptor competition binding experiments were carried out in membranes from HEK-293-A_{2B} cells (Euroscreen, Gosselies, Belgium) labeled with 35 nM [³H]DPCPX. Non-specific binding was determined in the presence of 400 μ M NECA. The reaction mixture was incubated at 25 °C for 30 min.

6.4.1.4. Human A₃ receptors. Adenosine A₃ receptor competition binding experiments were carried out in membranes from HeLa-A₃ cells. Labeled with 30 nM [³H]NECA. Non-specific binding was determined in the presence of 100 μ M (R)-PIA. The reaction mixture was incubated at 25 °C for 180 min.

After each incubation time samples were filtered and measured in a microplate beta scintillation counter (Microbeta Trilux, Perkin-Elmer, Madrid, Spain).

6.4.2. Isolated organ assays

6.4.2.1. A_{2A} receptors. These assays were performed in A_{2A} receptors³⁹ from isolated aorta of 200–250 g male Wistar-Kyoto rats as previously described.¹⁶

6.4.2.2. A_{2B} receptors. These assays were performed in A_{2B} receptors⁴⁰ isolated colon of 200–250 g male Wistar-Kyoto rats as previously described.¹⁶

Acknowledgements

The Italian authors thank the MIUR (Ministero dell'Istruzione, dell'Università e della Ricerca Scientifica, Rome-Italy) for financial support (PRIN Project 2006). The Spanish authors thank the Health Institute Carlos III (RD07/0067/0002) and Xunta de Galicia (07CSA003203PR) for partial financial support. J.B. is a recipient of a financial support from the Programa Isabel Barreto (Xunta de Galicia).

References and notes

- Fredholm, B. B.; Iljerman, A. P.; Jacobson, K. A.; Klotz, K. N.; Linden, J. *Pharmacol. Rev.* **2001**, *53*, 527.
- Jacobson, K. A.; Gao, Z.-G. *Nat. Rev. Drug Disc.* **2006**, *5*, 247.
- Moro, S.; Gao, Z.-G.; Jacobson, K. A.; Spalluto, G. *Med. Res. Rev.* **2006**, *26*, 131.
- Akkari, R.; Burbiel, J. C.; Hockemeyer, J.; Müller, C. E. *Curr. Top. Med. Chem.* **2006**, *6*, 1375.
- Jacobson, K. A.; Iljerman, A. P.; Linden, J. *Drug Dev. Res.* **1999**, *47*, 45.
- Holgate, S. T. *Br. J. Pharmacol.* **2005**, *145*, 1009.
- Tabrizi, M. A.; Baraldi, P. G.; Preti, D.; Romagnoli, R.; Saponaro, G.; Baraldi, S.; Moorman, A. R.; Zaid, A. N.; Varani, K.; Borea, P. A. *Bioorg. Med. Chem.* **2008**, *16*, 2419.
- Baraldi, P. G.; Tabrizi, M. A.; Preti, D.; Bovero, A.; Romagnoli, R.; Fruttarolo, F.; Zaid, N. A.; Moorman, A. R.; Varani, K.; Gessi, S.; Merighi, S.; Borea, P. A. *J. Med. Chem.* **2004**, *47*, 1434.
- Volpini, R.; Costanzi, S.; Vittori, S.; Cristalli, G.; Klotz, K. N. *Curr. Top. Med. Chem.* **2003**, *3*, 427.
- Kim, Y. C.; Ji, X.; Melman, N.; Linden, J.; Jacobson, K. A. *Drug Dev. Res.* **1999**, *47*, 178.
- Kim, Y. C.; Ji, X.; Melman, N.; Linden, J.; Jacobson, K. A. *J. Med. Chem.* **2000**, *43*, 1165.
- Vidal, B. J.; Esteve Trias, C.; Segarra Matamoros, V.; Ravina Rubira, E.; Fernandez Gonzales, F.; Loza Garcia, M. I.; Sanz Carreras, F.; WO Patent 03/000694, 2003.
- Carotti, A.; Stefanachi, A.; Ravina, E.; Sotelo, E.; Loza, M. I.; Cadavid, M. I.; Centeno, N. B.; Nicolotti, O. *Eur. J. Med. Chem.* **2004**, *39*, 879.
- Carotti, A.; Cadavid, M. I.; Centeno, N. B.; Esteve, C.; Loza, M. I.; Martinez, A.; Nieto, R.; Ravina, E.; Sanz, F.; Segarra, V.; Sotelo, E.; Stefanachi, A.; Vidal, B. *J. Med. Chem.* **2006**, *49*, 282.
- Stefanachi, A.; Brea, J. M.; Cadavid, M. I.; Centeno, N. B.; Esteve, C.; Loza, M. I.; Martinez, A.; Nieto, R.; Raviña, E.; Sanz, F.; Segarra, V.; Sotelo, E.; Vidal, B.; Carotti, A. *Bioorg. Med. Chem.* **2008**, *16*, 2852.
- Stefanachi, A.; Nicolotti, O.; Leonetti, F.; Cellamare, S.; Campagna, F.; Loza, M. I.; Brea, J. M.; Mazza, F.; Gavuzzo, E.; Carotti, A. *Bioorg. Med. Chem.* **2008**, *16*, 9780.
- Grahner, B.; Winiwarter, S.; Lanzner, W.; Müller, C. E. *J. Med. Chem.* **1994**, *37*, 1526.
- Hayallah, A. M.; Sandoval-Ramirez, J.; Reith, U.; Schobert, U.; Preiss, B.; Schumacher, B.; Daly, J. W.; Müller, C. E. *J. Med. Chem.* **2002**, *45*, 1500–1510.
- Elzein, E.; Kalla, R.; Li, X.; Perry, T.; Gimbel, A.; Zeng, D.; Lustig, K.; Leung, K.; Zablocki, J. *J. Med. Chem.* **2008**, *51*, 2267.
- Esteve, C.; Nueda, A.; Diaz, J. L.; Beleta, J.; Cardenas, A.; Lozoya, E.; Cadavid, M. I.; Loza, M. I.; Ryder, H.; Vidal, B. *Bioorg. Med. Chem. Lett.* **2006**, *51*, 3642.
- Stefanachi, A.; Leonetti, F.; Cappa, A.; Carotti, A. *Tetrahedron Lett.* **2003**, *44*, 2121.
- Papesch, V.; Dobson, R. M. G. D. *J. Org. Chem.* **1963**, *28*, 1329.
- Senda, S.; Suzui, A.; Honda, M.; Fujimura, H. *Chem. Pharm. Bull.* **1958**, *6*, 482.
- Totleben, M. J.; Freeman, J. P.; Szuszkowicz, J. *J. Org. Chem.* **1997**, *62*, 7319.
- D'Addona, D.; Bochet, C. G. *Tetrahedron Lett.* **2001**, *42*, 5227.

26. Yan, L.; Bertarelli, D. C.; Hayallah, A. M.; Meyer, H.; Klotz, K. N.; Müller, C. E. *J. Med. Chem.* **2006**, 49, 4384.
27. BioByte Corp., Claremont, CA, USA.
28. Advanced Chemistry Development, Toronto, Canada.
29. The Cambridge Crystallographic Data Centre via http://www.ccdc.cam.ac.uk/data_request/cif.
30. Pedretti, A.; Villa, L.; Vistoli, G. *J. Mol. Graph. Model.* **2002**, 21, 47.
31. Goodford, P. J. *J. Med. Chem.* **1985**, 28, 849.
32. Majer, P.; Randad, R. S. *J. Org. Chem.* **1994**, 59, 1937.
33. Prats, M.; Gálvez, C. *Heterocycles* **1991**, 34, 149.
34. Mohamadi, F.; Richards, N. G. J.; Guida, W. C.; Liskamp, R.; Lipton, M.; Caufield, C.; Chang, G.; Hendrikson, T.; Still, W. C. *J. Comput. Chem.* **1990**, 11, 440.
35. Jorgensen, W. L.; Tirado-Rives, J. *J. Am. Chem. Soc.* **1988**, 110, 1657.
36. Jorgensen, W. L.; Maxwell, D. S.; Tirado-Rives, J. *J. Am. Chem. Soc.* **1996**, 118, 11225.
37. MATLAB The Language of Technical Computing, version 7.3; The Mathworks: Natick, MA, USA, 2006.
38. Stewart, J. J. P. *Quant. Chem. Prog. Exch.* **1990**, 10, 86.
39. Prentice, D. J.; Hourani, S. M. O. *Br. J. Pharmacol.* **1996**, 118, 1509.
40. Fozard, J. R.; Baur, F.; Wolber, C. *Eur. J. Pharmacol.* **2003**, 475, 79.